



Thermoplastic Starch Nanocomposites Reinforced with Cellulose Nanocrystal Suspensions Containing Residual Salt from Neutralization

Christoph Metzger* and Heiko Briesen*

Sulfuric acid-catalyzed hydrolysis of cellulose commonly isolates cellulose nanocrystals (CNCs). Neutralizing the reactant solution with sodium hydroxide facilitates efficient downstream processing, but residual salt remains in the product. This study examines the reinforcing effects of CNCs from suspensions that contain residual salt on the mechanical properties of thermoplastic starch nanocomposites. By reinforcing starch films with up to 5 wt% CNCs, stiffness and strength are improved by 118% and 79%, respectively, indicating a good dispersion of CNCs in the starch matrix. Compared to nanocomposites incorporating salt-free CNCs, the remaining salt has no significant impact on the material's mechanical performance. The results indicate great potential of CNCs containing residual salt as biobased, low-cost nanofiller in hydrophilic polymer matrices.

is greater than that of polystyrene;^[13] nevertheless, the mechanical properties of polyethylene terephthalate and polycarbonate are still superior to those of PLA.^[14] Generally, biodegradable polymers from renewable resources, such as PLA, polyhydroxybutyrate, polycaprolactone, and polyhydroalkanoate, underperform regarding their mechanical and barrier properties.^[1,15] Furthermore, natural biopolymers, such as starch, chitosan, and alginate, show fast degradation and deteriorating mechanical properties in humid environment due to their prevalently hydrophilic character.^[7,16]


In nature, single materials' restraints are compensated for by forming composites, often with building blocks of nanoscale dimensions.^[17] Modern manufactured

1. Introduction

Many polymeric materials for everyday's use in key application areas, such as packaging, health care, electronics, automotive, and aerospace, are derived from petroleum.^[1–5] However, contemporary profuse consumption of petroleum and the lack of sustainable disposal possibilities introduce ecological concerns at petroleum-derived materials.^[1,6,7] Consequently, increasing efforts have been made toward the development of biopolymeric materials with properties that are tailored to particular applications.^[8–10] Biopolymers are produced from abundant resources, biodegradable and environmentally benign.^[11,12] However, individual biopolymers cannot compete with or exceed the performance of well-advanced thermoplastics derived from petroleum. For example, polylactic acid's (PLA) toughness

materials in engineering applications benefit from the same principles: composites containing nanoscale building blocks, for example organic–inorganic nanocomposites from sol–gel chemistry or carbon black reinforced elastomers, were in use long before even being referred to as nanotechnology.^[18] Since the mid-1990s, there has been a steady increase in published research addressing nanocomposites made from nanofillers dispersed in polymer matrices.^[19] Conforming to this principle, blends of biopolymers and nanofillers yield materials with improved properties for specific use cases.^[1,7,13,20] Depending on the nanofillers' inherent properties, they provide improved mechanical, barrier, and thermal properties to the nanocomposite.^[21,22] Furthermore, nanocomposite properties are, among others, strongly dependent on the filler's composition, aspect ratio, and surface properties.^[7,21,23–25] Increasing awareness of ecological problems has drawn attention to synthetic bionanocomposites with additional functionalities, such as biodegradability, biocompatibility, and renewability.^[26–29] In this context, the low cost and wide availability of starch from several renewable resources make it an interesting candidate for biodegradable products in packaging,^[30,31] which is reflected in the high number of original research articles and patents on the material.^[19] However, there is only a limited number of applications because of the low mechanical strength of starch and starch films' high gas permeation.^[32] Addition of nanofillers, such as silicates, carbon-based nanomaterials, or metal nanoparticles can improve the biopolymer's functional properties.^[18] Moreover, nanofillers from biopolymers, such as cellulose nanocrystals (CNCs), chitin nanocrystals, or starch nanoplatelets, make composites fully biodegradable,

C. Metzger, Prof. H. Briesen
TUM School of Life Sciences Weihenstephan
Chair of Process Systems Engineering
Technical University of Munich
Gregor-Mendel-Str. 4, 85354 Freising, Germany
E-mail: christoph.metzger@tum.de; briesen@wzw.tum.de

 The ORCID identification number(s) for the author(s) of this article can be found under <https://doi.org/10.1002/mame.202100161>

© 2021 The Authors. Macromolecular Materials and Engineering published by Wiley-VCH GmbH. This is an open access article under the terms of the Creative Commons Attribution License, which permits use, distribution and reproduction in any medium, provided the original work is properly cited.

DOI: 10.1002/mame.202100161

offering great potential for food packaging.^[17,18,26–29,32] In particular, CNCs' high axial elastic modulus, low density, and low-cost potential make them a promising candidate to improve the overall properties of starch-based nanocomposites.^[33] For that purpose, the large number of hydroxy groups on the CNC surfaces promotes hydrophilicity and, therefore, good dispersibility in a hydrophilic starch matrix.^[34–36] Hence, incorporation of CNCs in the starch matrix yields improved mechanical properties, which are promoted by good interfacial bonding, percolation network formation, and an increase of the system's crystallinity.^[33,37–42] A concurrent increase of the glass transition temperature expands the useful temperature range of CNC-starch nanocomposites.^[39,40,43–47] In addition, CNCs constrain swelling of starch and impede water diffusion through the nanocomposite.^[39,46,48–51] Considering macroscopic stiffness and strength of low-modulus polymers, CNCs are typically added to starch at low mass fractions < 30 wt% to improve the nanocomposite's mechanical properties.^[21,52] In this regard, it has been shown that volume fractions of about 1% already promote a continuous path of connected CNCs through the polymer matrix.^[52] In contrast, CNC aggregation occurs at elevated mass fractions, which results in reduced matrix homogeneity and limited interfacial cohesion and, thus, decremented overall performance.^[31,44]

CNC performance in nanocomposites strongly depends on the pathway used for their production as well as the cellulose source.^[53] Commonly, CNCs are produced by the sulfuric acid-catalyzed hydrolysis of cellulosic feedstock, yielding rod-shaped particles with a diameter of 3–50 nm and an aspect ratio between 5 and 50.^[54] Concurrent sulfation by grafting sulfate half-esters onto the CNCs induces a negative surface charge, resulting in stable colloidal suspensions in polar media.^[55] This well-studied laboratory procedure has a high potential for the pilot- and industrial-scale top-down production of CNCs.^[56,57] However, product separation from an acidic reactant solution necessitates low-efficiency techniques, such as dialysis or reverse osmosis.^[58] Overall, a more energy- and resource-efficient production method is required to successfully commercialize CNCs.^[59]

In this context, Metzger et al. designed an economic separation process to produce colloiddally stable CNCs from neutralized reactant solutions.^[60] After hydrolysis, the reactant solution is neutralized with a base, such as sodium hydroxide, to form a secondary sulfate (Na_2SO_4). Successive centrifugation steps remove excess ions and by-products until peptization occurs. Critical concentrations for agglomeration and peptization are independent of CNC mass fraction. Hence, the amount of salt in the product can be controlled by adjusting the amount of water added before and after each washing step.^[60,61] Eventually, a stable colloidal suspension is formed by diluting the product to a salt concentration below the critical agglomeration concentration.

Cost-effective CNC production via neutralization of the acidic reactant solution facilitates commercialization efforts by overcoming economic market barriers.^[56,58] Thus far, we have reported the effect of different sulfate salts on colloidal CNCs isolated by this process.^[60] Furthermore, we have successfully applied CNC suspensions containing residual salt from neutralization as an oxygen barrier layer in polymer films.^[62] Complementary to these reported works, we hypothesize in this study that CNC suspensions containing residual salt have mechanical

reinforcing ability in starch nanocomposites similar to salt-free CNCs. For this purpose, CNCs were isolated from cotton cellulose by sulfuric acid-catalyzed hydrolysis, and suspensions with and without residual sulfate salt were prepared. Effects of CNCs with and without residual salt on the mechanical performance of CNC-starch nanocomposites were comparatively investigated. CNCs containing residual salt, but having similar performance to salt-free CNCs, offer great potential as a biobased, low-cost filler in sustainable nanocomposites.

2. Results and Discussion

2.1. Disperse Properties of Colloidal CNCs

Suspensions of salt-free CNCs (D-CNCs) and salt-containing CNCs (S-CNCs) were prepared by sulfuric acid-catalyzed hydrolysis of cotton α -cellulose, neutralization with NaOH, and peptization after removing the salt by centrifugation. As previously reported, the applied CNC isolation protocol yields particles with mean length of 120 nm and diameters ≤ 10 nm, which have been determined by transmission electron microscopy.^[60] S-CNCs had a salt content of 12.8 ± 0.2 mg Na_2SO_4 g^{-1} CNC (90×10^{-3} M). D-CNCs were further dialyzed to remove the remaining salt from the product. Dynamic light scattering (DLS) and electrophoretic light scattering (ELS) were used to determine hydrodynamic apparent particle diameter (z -avg) and zeta potential of CNCs in each sample, respectively. In accordance with our previous study,^[60] z -avg of D-CNCs and S-CNCs was 202 ± 3 and 227 ± 5 nm, respectively, which is in the average range of CNCs of 50–200 nm.^[63] Larger hydrodynamic apparent particle diameter of S-CNCs indicated salt-induced cluster formation of CNCs in the presence of Na_2SO_4 .^[64] Furthermore, D-CNCs and S-CNCs showed zeta potentials of -44.3 ± 4.9 mV and -35.5 ± 7.6 mV, respectively. All values were in the commonly reported range of -50 to -20 mV of sulfated CNCs and indicated elevated colloidal stability of D-CNCs in the salt-free suspension.^[63,65]

2.2. Characterization of Starch-Based Nanocomposites

Starch-based nanocomposites containing D-CNCs or S-CNCs as reinforcing fillers at mass fractions of 1, 2, and 5 wt% were prepared by solution casting. Bare starch-glycerol films were used as the reference material. The effects of salt on the starch-glycerol films' mechanical properties were also evaluated by casting starch-glycerol films containing equivalent Na_2SO_4 contents to that in S-CNC suspensions. The mass fraction of glycerol as a plasticizer in all formulations was maintained at 30 wt%.

Table 1 shows the mean thickness of starch films and starch-based nanocomposites after conditioning at a relative humidity of 44%. Based on the dry mass of the respective constituents, a thickness of 75 μm was targeted for all films; however, actual film thicknesses exceeded the targeted value due to moisture uptake of the hygroscopic constituents.^[66,67] Note that nanocomposites containing S-CNCs and D-CNCs have higher film thicknesses compared to bare starch films and starch films containing Na_2SO_4 . Nevertheless, no significant impact of CNC or salt mass fraction on film thickness is deductible from the results shown in Table 1.

Table 1. Mean thickness of starch films and starch-based nanocomposites at a relative humidity of 44%.

Equivalent CNC mass fraction [wt%]	0	1	2	5
Constituents	Mean film thickness [μm]			
Starch	90 \pm 5			
Starch + Na ₂ SO ₄		87 \pm 4	88 \pm 8	88 \pm 4
Starch + S-CNCs		98 \pm 8	92 \pm 7	97 \pm 5
Starch + D-CNCs		96 \pm 7	95 \pm 6	98 \pm 8

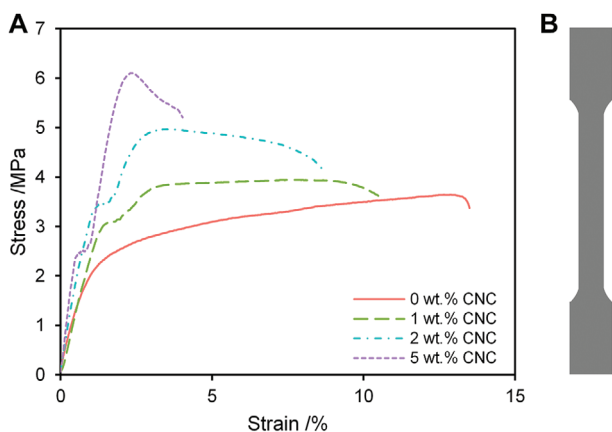


Figure 1. a) Representative stress–strain curves of starch-glycerol films and starch-CNC nanocomposites with different contents of S-CNCs. b) Specimen geometry for uniaxial tensile testing (not to scale), according to ISO 527-3.^[73]

The impact of S-CNCs on the mechanical properties of starch nanocomposites is shown in **Figure 1a** and the specimen geometry of all tensile-tested samples is illustrated in **Figure 1b**. Increasing the filler content caused both strengthening and stiffening of the nanocomposites, recognizable by the increased ultimate tensile strength and Young’s modulus, respectively. At the same time, uniform strain and elongation at failure decreased and,

hence, increasing the filler content induced a decrease in ductility. These effects are mainly attributable to the formation of a rigid CNC network in the nanocomposite.^[31] Concurrently, mutual entanglement of CNCs and starch, as well as efficient stress transfer from the starch matrix to the nanofiller, promotes improvement of the nanocomposite’s mechanical properties, at the expense of ductility.^[37,38,68–72] In addition, it has been reported that CNCs have a nucleating effect on the matrix, which causes an increase of the system’s overall crystallinity.^[39,40,46,47]

Figure 2 shows the mechanical properties of starch films and starch-CNC nanocomposites prepared by all formulations. Overall, the addition of Na₂SO₄ at equivalent salt contents \leq 5 wt% S-CNCs had no significant impact on the mechanical properties of starch films. Thus, addition of salt at the given concentrations did not alter force transmission within the starch matrix. In contrast, addition of CNCs as nanofiller increased the material’s stiffness, while its plastic deformation was constrained. To that effect, the nanocomposites’ resistance to elastic deformation increased with increasing filler content, as determined by the increasing Young’s modulus from 1.57 \pm 0.23 MPa at 0 wt% CNC to 3.42 \pm 0.14 MPa at 5 wt% CNC for S-CNCs (+118%) (**Figure 2a**). As expected, the mechanical properties of the nanocomposites lie between those of bare starch and CNCs, with CNCs having a Young’s modulus in the range of 100–130 GPa.^[74] Similar to the addition of S-CNCs, addition of 5 wt% D-CNCs increased Young’s modulus to 3.63 \pm 0.40 MPa (+132%). Although S-CNCs had a lesser effect on the nanocomposites’ stiffness than D-CNCs, both were within the corresponding confidence intervals and, hence, residual salt did not significantly affect the elastic behavior of starch-CNC nanocomposites. **Figure 2b** shows the evolution of ultimate tensile strength as a function of filler content. A filler content of 5 wt% elevated the ultimate tensile strength of the nanocomposites from 3.55 \pm 0.79 MPa to 6.35 \pm 0.41 MPa (+79%) and 6.59 \pm 0.67 MPa (+86%) for S-CNCs and D-CNCs, respectively. Therefore, CNCs strengthened the material by increasing the maximum bearable stress it can endure before failure occurs; however, filler contents of 1 and 2 wt% had no significant impact on σ_{UTS} for both S-CNCs and D-CNCs. Again, S-CNCs show marginally inferior performance compared to D-CNCs; but no significant

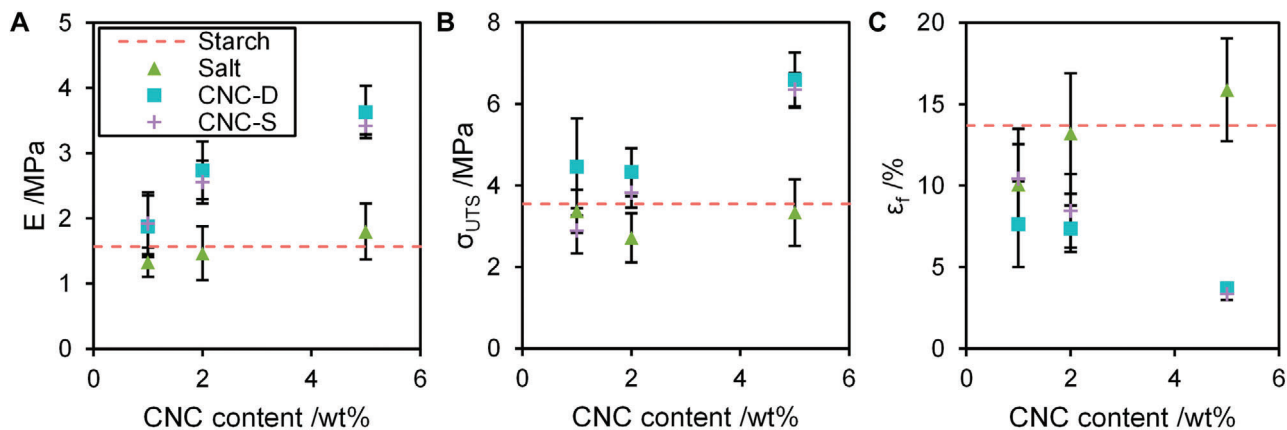


Figure 2. Mechanical properties in terms of a) Young’s modulus, b) ultimate tensile strength, and c) elongation at fracture of bare starch films, starch films with equivalent amounts of salt as in S-CNCs, and starch nanocomposites containing D-CNCs or S-CNCs at different filler contents.

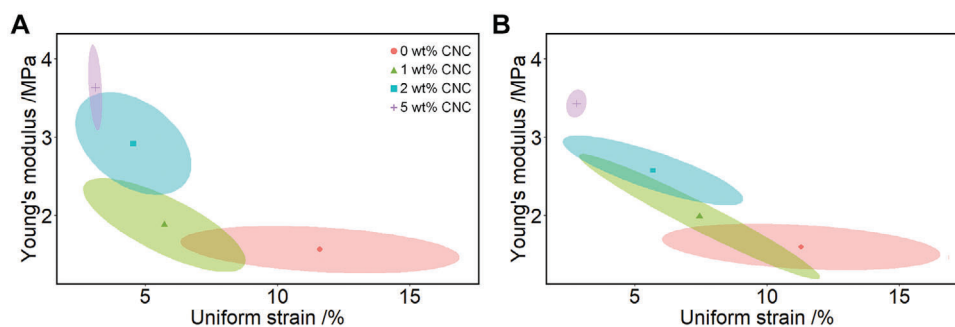


Figure 3. Young's modulus as a function of uniform strain at different filler contents of a) D-CNC or b) S-CNC. The points denote the respective mean values and the ellipses represent the confidence intervals of the means.

difference was found between nanocomposites containing each filler. Furthermore, addition of CNCs to the starch matrix made the nanocomposites more brittle. This is indicated by the reduced elongation at failure, which decreases from $13.7 \pm 3.9\%$ to $3.4 \pm 0.4\%$ (-75%) for S-CNCs and $3.7 \pm 0.4\%$ (-73%) for D-CNCs, respectively (Figure 2c). Overall, the effect of both S-CNCs and D-CNCs on the mechanical properties of starch nanocomposites did not deviate at given CNC mass fractions and, hence, no significant impact of residual salt in CNC suspensions was concluded. Furthermore, the observed increase in strength and concurrent decrease of ductility of starch-CNC nanocomposites lies well within the ranges that have been reported for the relative change of each property.^[70,75,76]

Figure 3 presents Young's modulus and uniform strain for starch nanocomposites containing D-CNCs (Figure 3a) or S-CNCs (Figure 3b) at different filler contents. This figure provides a better understanding of the effects of CNCs on the mechanical properties of starch-based nanocomposites. A power law-behavior can approximate the filler content's effect of both D-CNCs and S-CNCs. Stiffness increased with increasing filler content and ductility decreased. Hence, interfacial binding of the hydrophilic CNCs in the starch matrix was good.^[31] Note that commonly a linear relationship of Young's modulus and the filler content is determined.^[70] In comparison, power law-behavior represents a reinforcing effect in accordance with the percolation model by Favier et al.^[52]

Overall, nanocomposites containing S-CNCs exhibit marginally lower stiffness and higher brittleness than D-CNCs at equal filler contents. This effect is tentatively explained by CNC cluster formation in the presence of salt and, therefore, lower aspect ratio.^[24] However, both fillers' conformable confidence intervals indicate that the salt content of S-CNCs had no significant impact on the mechanical properties of the resulting starch-based nanocomposites.

2.3. Scanning Electron Microscopy Imaging and Fractography

Figure 4a,b shows scanning electron microscopy (SEM) images on the surface morphology of a) a starch film and b) a starch-CNC nanocomposite film containing 5 wt% S-CNCs, which both contain 30 wt% glycerol as plasticizer. Both films have no pores or cracks; however, the microscopic surface structure indicates the presence of nonplasticized starch granules. Generally, glycerol is

well suited to plasticize starches with high amylose content, such as corn starch.^[66,77–79] Nevertheless, some authors recommend plasticizer concentrations > 30 wt% to fully dissolve starch granules and, thus, achieve homogeneous starch films with smooth surface.^[66,79] Addition of CNCs containing residual salt and salt-free CNCs (not shown here) have no impact on the surface microstructure of the nanocomposite films.

The fracture pattern of starch-CNC composites was analyzed by SEM using tensile-tested specimens. Figure 4b,c presents SEM images in the vicinity of the fracture sites, indicating that cracks occurred perpendicular to the force vector before failure. No cracks occurred further from the fracture edge. Qualitatively, the distorted texture at the surface of starch-glycerol films implies higher ductility; and the number of perpendicularly oriented cracks decreased as filler content increased. However, there was no assessable difference between the samples containing S-CNCs or D-CNCs.

3. Conclusion

This study evaluated the reinforcing effect of CNCs on starch-based nanocomposite films at filler contents ≤ 5 wt%. We devoted particular attention to CNCs containing residual salt from an efficient neutralization-based isolation process (S-CNCs). Salt-free CNCs from dialyzed suspensions (D-CNCs) were used for immediate comparison. The results confirmed the reinforcing effect of CNCs on the nanocomposite's mechanical properties from the increase in stiffness and strength of the material with increasing CNC content; with a concomitant decrease in ductility. In detail, addition of 5 wt% S-CNCs led to an increase of the material's stiffness by 118% and ultimate tensile strength increased by 79%. The improvement of the mechanical properties was at the expense of ductility and elongation at fracture decreased by 75% concurrently. Although the results indicated a good overall dispersion of CNCs in the starch matrix, we assumed that residual salt induces CNC cluster formation. Consequently, reinforcement of starch-based nanocomposites with CNCs containing residual salt resulted in marginally lower performance compared to nanocomposites reinforced with salt-free CNCs. The difference between S-CNCs and D-CNCs was overall $< 6.1\%$ and statistically not significant. In conclusion, these results will be of particular interest for the production of low-cost, high-volume nanocomposites based on hydrophilic and thermoplastic polymers.

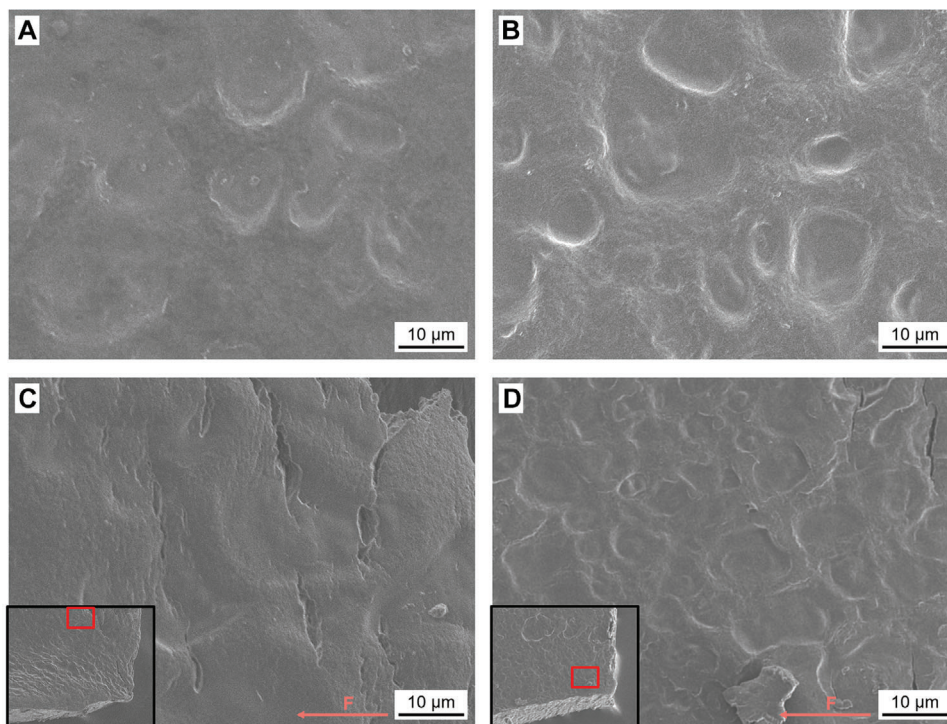


Figure 4. Surface of a) bare starch-glycerol and b) a starch-based nanocomposite film containing 5 wt% S-CNCs at 1000x magnification; and surface of tensile-tested specimens in the vicinity of the fracture of c) a bare starch-glycerol film and d) a starch-based nanocomposite film containing 5 wt% S-CNCs. The arrows indicate the vector of a unidirectionally applied force. The rectangles in the images at the left bottom corners indicate the location of the magnified images. Here, the fracture edge is located at the right side and the sample edge at the bottom.

4. Experimental Section

Reagents: Whatman ashless filter aids (cotton α -cellulose; water content 5 wt%) were purchased from Sigma-Aldrich (Taufkirchen, Germany). Corn starch (water content 15 wt%), glycerol (99.5%), potassium carbonate (K_2CO_3 , 99%), and sodium hydroxide (NaOH, 99%) were purchased from Carl Roth (Karlsruhe, Germany). Sulfuric acid (H_2SO_4 , 95%) was obtained from VWR (Ismaning, Germany). All chemicals were used as received. Ultrapure (type 1) water with a resistivity of 18.2 M Ω cm (Milli-Q Direct 8 system, Merck Chemicals, Schwalbach, Germany) was used in all experiments.

Preparation of CNC Suspensions: Sulfated CNCs were extracted from cotton α -cellulose by sulfuric acid-catalyzed hydrolysis using the method reported by Cranston and Gray,^[80] followed by neutralization with NaOH, according to the methodology reported by Metzger et al.^[60,62] and Müller and Briesen.^[81] Cellulose was oven-dried for 30 min at 105 °C to evaporate adsorbed water. Dried cellulose was then mixed with preheated sulfuric acid (64 wt%) at 45 °C at an acid-to-cellulose ratio of 10 and stirred for 45 min. Average CNC dimensions resulting from the applied process conditions are 120 nm in length and ≤ 10 nm in diameter, determined by transmission electron microscopy.^[60] The reaction was stopped by transferring the reaction solution to an ice bath, followed by incremental neutralization of 85 mol% of the initially provided acid with ice-cold NaOH (aq) (1.25 M). The intermediate product was washed by twofold centrifugation for 15 min at 4500 \times g (Centrifuge 5804 R, Eppendorf, Hamburg, Germany), decanted, and diluted. After the first washing step, NaOH (s) was added to adjust the pH to 7 and the amount of water added was adjusted to 110% of the critical peptization concentration of 115×10^{-3} M.^[60] After the second washing step, the sample was concentrated by vacuum evaporation (Rotavapor R 100, Büchi, Essen, Germany) to a salt concentration above the critical agglomeration

concentration and ultrasonicated with a VS 70 T sonotrode (Sonopuls HD 3400, Bandelin, Berlin, Germany) in an ice bath at an input energy of 5 kJ g⁻¹ cellulose and a power of 33.3 W. After ultrasonication, incompletely hydrolyzed cellulosic residues were removed by centrifugation. The sample denoted as S-CNC was stored at 4 °C until further use. A portion of the sample was dialyzed in regenerated cellulose tubes with a molecular weight cutoff of 12–14 kDa (ZelluTrans/ROTH T3, Carl Roth, Karlsruhe, Germany) for 7 d against running water to remove the remaining salt and soluble by-products. The dialyzed sample was denoted as D-CNC.

Plasticized Starch Nanocomposites: Pure starch-glycerol films, nanocomposite films incorporating D-CNCs or S-CNCs, and starch-glycerol films incorporating Na_2SO_4 were prepared by solution casting, as described previously.^[62,82] Water was preheated to 70 °C in a water bath. Starch was then added and the suspension was stirred for 1 h to allow gelatinization. D-CNCs, S-CNCs, or salt and glycerol were added, and stirring was continued for 30 min to allow plasticization and mixing of the diluted composite. All precursor solutions with the total mass, m_{total} , had a water content, w_{H_2O} , of 97 wt%. The glycerol weight fraction, w_{gly} , was kept constant at 30 wt% with respect to the solid fraction. The nanoparticle loading, w_{CNC} , was varied between 1 and 5 wt% concerning the solid fraction. Residual salt in the S-CNCs was considered in the calculations. The mass fraction of salt, w_{salt} , added to starch-glycerol films was matched with the salt content of the films incorporating S-CNCs. The weighed mass of each chemical was calculated using Equation (1), considering the weight of starch, m_{starch} , and water added, m_{H_2O} , and corrected for the water content of each component

$$m_{total} = (1 + w_{gly} + w_{CNC} + w_{salt}) \cdot m_{starch} + w_{H_2O} \cdot m_{H_2O} \quad (1)$$

The filmogenic solutions were homogenized in a low-intensity ultrasonic bath for 3 min to remove bubbles and then cast in polystyrene



Petri dishes (Greiner Bio-One, distributed by VWR, Ismaning, Germany). The target dry film thickness was 75 μm . Excess water was evaporated overnight in a climatic chamber (ICH 110, Memmert, Schwabach, Germany) at 40 °C with a relative humidity of 47%. The films were then turned upside down for double-sided drying overnight. Before use, all films were conditioned in a desiccator over a saturated K_2CO_3 solution at 23 °C, resulting in a constant relative humidity of 44%.

Characterization of the CNCs and Nanocomposites: Dry Mass and Salt Content: The dry constituents' mass fractions at different production stages were calculated using an aliquot's mass fraction before and after water evaporation by lyophilization (2-4 LSCplus, Christ, Osterode am Harz, Germany). Then, the sample's cellulosic fraction was extrapolated from the mass fraction in the aliquots. The yield refers to the initially provided amount of cellulose, considering the overall mass balance and losses of particular unit operations.

Light Scattering Techniques: The hydrodynamic apparent particle diameter of the CNCs was measured by DLS using a Zetasizer Nano ZSP (Malvern Instruments, Worcestershire, UK). Aliquots of D-CNCs and S-CNCs were filtered through syringe filters with a glass fiber membrane and a pore size of 1 μm (Chromafil Xtra GF, Macherey-Nagel, Düren, Germany). The harmonic intensity-averaged particle diameter ($z\text{-avg}$) from the cumulants analysis was obtained for 0.025 wt% CNC suspensions after equilibration for 3 min at 25 °C. Zeta potentials of D-CNCs and S-CNCs were determined by ELS using the same instrument. Aliquots were similarly filtered, diluted to 0.25 wt%, and equilibrated.

Mechanical Properties: Uniaxial tensile tests were carried out on a zwickLine Z2.5 testing machine (ZwickRoell, Ulm, Germany) according to the standards of the International Organization for Standardization (ISO), ISO 527-1 and ISO 527-3, using screw grips, equivalent to ZwickRoell type 8133.^[73,83] Specimens were cut from individual films in a random orientation with a length of 125 mm and a width of 26 mm in the reduced section. After a preload of 0.1 N, a constant extension rate of 25 mm min^{-1} was applied. Film thickness was mechanically measured on three evenly distributed measuring points in the reduced section, using the thickness closest to the point of fracture for stress calculations. Ultimate tensile strength, σ_{UTS} , uniform strain, ϵ_{UTS} , at σ_{UTS} , and the elongation at failure, ϵ_f , were read from the stress-strain curve, σ versus ϵ . Young's modulus, E , was evaluated according to Hooke's law from the linear-elastic relationship in the initial region of the stress-strain curve (Equation (2))

$$E = \frac{\sigma}{\epsilon} \quad (2)$$

SEM Imaging: The film morphology was examined using a JEOL JSM-IT100 scanning electron microscope (Akishima, Japan) with a secondary electron detector at an acceleration voltage of 3 kV. The films were mounted on conducting carbon tape.

Remarks: The weighed mass of each chemical in the experimental section refers to their dry state. Their water content, indicated by the vendor or determined by gravimetric analysis, was considered in all calculations. All measurements were performed at least six times. The results are presented with a 95% confidence interval of the mean. The uncertainty of derived quantities depending on multiple variables is given by the propagation of error.

Acknowledgements

The authors wish to thank Sonja Kraus for performing the instructive preliminary tests and Walter Seidl to construct equipment for mechanical testing and Michael Gebhardt (Technical University of Munich, Chair of Zoology) for providing access to the scanning electron microscope. This research was funded by the Federal Ministry of Education and Research of Germany (Bundesministerium für Bildung und Forschung, BMBF) in the framework of the NanoCELL project within the funding initiative NanoCare 4.0 (Grant No. 03XP196A).

Open access funding enabled and organized by Projekt DEAL.

Conflict of Interest

The authors declare no conflict of interest.

Data Availability Statement

Research data are not shared.

Keywords

bionanocomposites, cellulose nanocrystals (CNCs), mechanical properties, mechanical reinforcement, nanocomposites, neutralization, thermo-plastic starch

Received: March 9, 2021

Revised: April 28, 2021

Published online: May 29, 2021

- [1] E. S. Medeiros, A. S. Santos, A. Dufresne, W. J. Orts, L. H. Mattoso, in *Polymer Composites, Biocomposites* (Eds: S. Thomas, K. Joseph, S. K. Malhotra, K. Goda, M. S. Sreekala), Wiley, Hoboken **2013**, p. 361.
- [2] J. G. Drobny, in *Applications of Fluoropolymer Films: Properties, Processing, and Products* (Ed: J. G. Drobny), William Andrew, Norwich **2020**, p. 3.
- [3] S. Gopi, P. Balakrishnan, D. Chandradhara, D. Poovathankandy, S. Thomas, *Mater. Today Chem.* **2019**, *13*, 59.
- [4] P. Balakrishnan, S. Gopi, M. S. Sreekala, S. Thomas, *Starch – Stärke* **2018**, *70*, 1700139.
- [5] F. M. Pelissari, D. C. Ferreira, L. B. Louzada, F. dos Santos, A. C. Corrêa, F. K. V. Moreira, L. H. Mattoso, in *Starches for Food Application* (Eds: M. T. P. Silva Clerici, M. Schmiele), Academic Press, New York, NY, USA **2019**, p. 359.
- [6] A. N. Netravali, S. Chabba, *Mater. Today* **2003**, *6*, 22.
- [7] L. Yu, K. Dean, L. Li, *Prog. Polym. Sci.* **2006**, *31*, 576.
- [8] P. Balakrishnan, V. G. Geethamma, M. S. Sreekala, S. Thomas, in *Fundamental Biomaterials: Polymers* (Eds: S. Thomas, P. Balakrishnan, M. S. Sreekala), Woodhead Publishing, Cambridge, Sawston, UK **2018**, p. 1.
- [9] P. Balakrishnan, M. S. Thomas, L. A. Pothan, S. Thomas, M. S. Sreekala, in *Encyclopedia of Polymeric Nanomaterials* (Eds: S. Kobayashi, K. Müllen), Springer, Berlin, Heidelberg, Germany **2019**, p. 1.
- [10] K. K. Sadasivuni, P. Saha, J. Adhikari, K. Deshmukh, M. B. Ahamed, J. -J. Cabibihan, *Polym. Compos.* **2020**, *41*, 32.
- [11] K. Van De Velde, P. Kiekens, *Polym. Test.* **2002**, *21*, 433.
- [12] D. L. Kaplan, in *Biopolymers from Renewable Resources* (Ed: D. L. Kaplan), Springer, Berlin, Heidelberg, Germany **1998**, p. 1.
- [13] K. Hamad, M. Kaseem, M. Ayyoob, J. Joo, F. Deri, *Prog. Polym. Sci.* **2018**, *85*, 83.
- [14] M. Biron, in *Thermoplastics and Thermoplastic Composites*, William Andrew, Waltham, MA, USA **2013**, p. 133.
- [15] S. Shankar, J. W. Rhim, in *Innovative Food Processing Technologies*, Elsevier, New York, NY, USA **2018**, p. 234.
- [16] E. Jamróz, P. Kulawik, P. Kopel, *Polymers* **2019**, *11*, 675.
- [17] A. Urvoas, M. Valerio-Lepiniec, P. Minard, C. Zollfrank, in *Bionanocomposites* (Eds: C. Aimé, T. Coradin), John Wiley and Sons, Inc., Hoboken, NJ **2017**, p. 1.
- [18] D. R. Paul, L. M. Robeson, *Polymer* **2008**, *49*, 3187.
- [19] *Concluded from manual keyword searches on Scopus and Web of Science.*
- [20] M. Mucha, S. Ludwiczak, M. Kawinska, *Carbohydr. Polym.* **2005**, *62*, 42.



- [21] R. J. Moon, A. Martini, J. Nairn, J. Simonsen, J. Youngblood, *Chem. Soc. Rev.* **2011**, *40*, 3941.
- [22] O. Faruk, A. K. Bledzki, H.-P. Fink, M. Sain, *Prog. Polym. Sci.* **2012**, *37*, 1552.
- [23] F. Luzi, L. Torre, J. M. Kenny, D. Puglia, *Materials* **2019**, *12*, 471.
- [24] A. Babaei-Ghazvini, B. Cudmore, M. J. Dunlop, B. Acharya, R. Bissessur, M. Ahmed, W. M. Whelan, *Carbohydr. Polym.* **2020**, *247*, 116688.
- [25] P. Balakrishnan, S. Gopi, V. G. Geethamma, N. Kalarikkal, S. Thomas, *Macromol. Symp.* **2018**, *380*, 1800102.
- [26] F. Li, E. Mascheroni, L. Piergiovanni, *Packag. Technol. Sci.* **2015**, *28*, 475.
- [27] B. Thomas, M. C. Raj, K. B. Athira, M. H. Rubiyah, J. Joy, A. Moores, G. L. Drisko, C. Sanchez, *Chem. Rev.* **2018**, *118*, 11575.
- [28] F. Vilarinho, A. Sanches Silva, M. F. Vaz, J. P. Farinha, *Crit. Rev. Food Sci. Nutr.* **2018**, *58*, 1526.
- [29] A. Dufresne, *Curr. For. Rep.* **2019**, *5*, 76.
- [30] E. S. Medeiros, A. Dufresne, W. J. Orts, in *Starches* (Ed: A. Bertolini), CRC Press, Boca Raton, FL, USA **2009**, p. 205.
- [31] F. Xie, E. Pollet, P. J. Halley, L. Avérous, in *Polysaccharides* (Eds: K. G. Ramawat, J.-M. Mérillon), Springer International Publishing, Cham **2021**, p. 1.
- [32] N. L. García, L. Famá, N. B. D'Accorso, S. Goyanes, in *Eco-Friendly Polymer Nanocomposites*, Vol. 75 (Eds: V. K. Thakur, M. K. Thakur), Springer India, New Delhi **2015**, p. 17.
- [33] Y. Habibi, L. A. Lucia, O. J. Rojas, *Chem. Rev.* **2010**, *110*, 3479.
- [34] J. Kim, G. Montero, Y. Habibi, J. P. Hinestroza, J. Genzer, D. S. Argyropoulos, O. J. Rojas, *Polym. Eng. Sci.* **2009**, *49*, 2054.
- [35] D. Klemm, F. Kramer, S. Moritz, T. Lindström, M. Ankerfors, D. Gray, A. Dorris, *Angew. Chem., Int. Ed. Engl.* **2011**, *50*, 5438.
- [36] S. Eyley, W. Thielemans, *Nanoscale* **2014**, *6*, 7764.
- [37] A. Kaushik, M. Singh, G. Verma, *Carbohydr. Polym.* **2010**, *82*, 337.
- [38] G. Siqueira, J. Bras, A. Dufresne, *Biomacromolecules* **2009**, *10*, 425.
- [39] A. P. Mathew, A. Dufresne, *Biomacromolecules* **2002**, *3*, 609.
- [40] A. P. Mathew, W. Thielemans, A. Dufresne, *J. Appl. Polym. Sci.* **2008**, *109*, 4065.
- [41] X. Ma, Y. Cheng, X. Qin, T. Guo, J. Deng, X. Liu, *LWT* **2017**, *86*, 318.
- [42] A. Kaushik, J. Kumra, *J. Elastomers Plast.* **2014**, *46*, 284.
- [43] X. Cao, Y. Chen, P. R. Chang, M. Stumborg, M. A. Huneault, *J. Appl. Polym. Sci.* **2008**, *109*, 3804.
- [44] Y. Chen, C. Liu, P. R. Chang, D. P. Anderson, M. A. Huneault, *Polym. Eng. Sci.* **2009**, *49*, 369.
- [45] Y. Lu, L. Weng, X. Cao, *Carbohydr. Polym.* **2006**, *63*, 198.
- [46] M. N. Anglès, A. Dufresne, *Macromolecules* **2000**, *33*, 8344.
- [47] M. N. Anglès, A. Dufresne, *Macromolecules* **2001**, *34*, 2921.
- [48] H. L. Luo, J. J. Lian, Y. Z. Wan, Y. Huang, Y. L. Wang, H. J. Jiang, *Mater. Sci. Eng., A* **2006**, *425*, 70.
- [49] M. S. Sreekala, K. Goda, P. V. Devi, *Compos. Interfaces* **2008**, *15*, 281.
- [50] A. J. Svagan, M. S. Hedenqvist, L. Berglund, *Compos. Sci. Technol.* **2009**, *69*, 500.
- [51] Y. Z. Wan, H. Luo, F. He, H. Liang, Y. Huang, X. L. Li, *Compos. Sci. Technol.* **2009**, *69*, 1212.
- [52] V. Favier, R. Dendievel, G. Canova, J. Y. Cavaille, P. Gilormini, *Acta Mater.* **1997**, *45*, 1557.
- [53] O. M. Vanderfleet, E. D. Cranston, *Nat. Rev. Mater.* **2021**, *6*, 124.
- [54] International Standardization Organization, ISO/TS 20477:2017, Nanotechnologies – Standard Terms and Their Definition For Cellulose Nanomaterial, (2017). <https://www.iso.org/standard/68153.html> (accessed: April 2021).
- [55] X. M. Dong, D. G. Gray, *Langmuir* **1997**, *13*, 2404.
- [56] C. A. De Assis, C. Houtman, R. Phillips, E. M. (T.) Bilek, O. J. Rojas, L. Pal, M. S. Peresin, H. Jameel, R. Gonzalez, *Biofuels, Bioprod. Biorefin.* **2017**, *11*, 682.
- [57] T. Lindstrom, *Tappi J.* **2019**, *18*, 308.
- [58] A. Rudie, in *Handbook of Nanocellulose and Cellulose Nanocomposites* (Eds: H. Kargarzadeh, I. Ahmad, S. Thomas, A. Dufresne), Wiley-VCH Verlag GmbH & Co. KGaA, Weinheim, Germany **2017**, p. 761.
- [59] C. S. Davis, D. L. Grolman, A. Karim, J. W. Gilman, *Green Mater.* **2015**, *3*, 53.
- [60] C. Metzger, D. Auber, S. Dähnhardt-Pfeiffer, H. Briesen, *Cellulose* **2020**, *27*, 9839.
- [61] T. Phan-Xuan, A. Thuresson, M. Skepö, A. Labrador, R. Bordes, A. Matic, *Cellulose* **2016**, *23*, 3653.
- [62] C. Metzger, S. Sanahuja, L. Behrends, S. Sänglerlaub, M. Lindner, H. Briesen, *Coatings* **2018**, *8*, 142.
- [63] E. J. Foster, R. J. Moon, U. P. Agarwal, M. J. Bortner, J. Bras, S. Camarero-Espinosa, K. J. Chan, M. J. D. Clift, E. D. Cranston, S. J. Eichhorn, D. M. Fox, W. Y. Hamad, L. Heux, B. Jean, M. Korey, W. Nieh, K. J. Ong, M. S. Reid, S. Renneckar, R. Roberts, J. A. Shatkin, J. Simonsen, K. Stinson-Bagby, N. Wanasekara, J. Youngblood, *Chem. Soc. Rev.* **2018**, *47*, 2609.
- [64] A. A. Moud, M. Arjmand, J. Liu, Y. Yang, A. Sanati-Nezhad, S. H. Hejazi, *Cellulose* **2019**, *26*, 9387.
- [65] A. Kumar, C. K. Dixit, in *Advances in Nanomedicine for the Delivery of Therapeutic Nucleic Acids* (Eds: S. Nimesh, R. Chandra, G. Nidhi), Woodhead Publishing, Cambridge, Sawston, UK **2017**, p. 43.
- [66] E. Basiak, A. Lenart, F. Debeaufort, *Polymers* **2018**, *10*, 412.
- [67] X. Guo, Y. Wu, X. Xie, *Sci. Rep.* **2017**, *7*, 14207.
- [68] A. Khan, R. A. Khan, S. Salmieri, C. Le Tien, B. Riedl, J. Bouchard, G. Chauve, V. Tan, M. R. Kamal, M. Lacroix, *Carbohydr. Polym.* **2012**, *90*, 1601.
- [69] H. Aloui, K. Khwaldia, M. Hamdi, E. Fortunati, J. M. Kenny, G. G. Buonocore, M. Lavgna, *ACS Sustainable Chem. Eng.* **2016**, *4*, 794.
- [70] Z. W. Abdullah, Y. Dong, *J. Mater. Sci.* **2018**, *53*, 15319.
- [71] V. Nessi, X. Falourd, J.-E. Maigret, K. Cahier, A. D'orlando, N. Descamps, V. Gaucher, C. Chevigny, D. Lourdin, *Carbohydr. Polym.* **2019**, *225*, 115123.
- [72] F. M. Pelissari, M. M. Andrade-Mahecha, P. J. D. A. Sobral, F. C. Menegalli, *J. Colloid Interface Sci.* **2017**, *505*, 154.
- [73] International Standardization Organization, ISO 527-3:2018, Plastics – Determination of Tensile Properties – Part 3: Test Conditions for Films and Sheets, (2018). <https://www.iso.org/standard/70307.html> (accessed: April 2021).
- [74] A. Dufresne, *Mater. Today* **2013**, *16*, 220.
- [75] A. Kaushik, R. Kaur, *Compos. Interfaces* **2016**, *23*, 701.
- [76] C. Balvino, N. Macke, R. Kato, S. J. Rowan, *Prog. Polym. Sci.* **2020**, *103*, 101221.
- [77] M. G. A. Vieira, M. A. Da Silva, L. O. Dos Santos, M. M. Beppu, *Eur. Polym. J.* **2011**, *47*, 254.
- [78] D. Domene-López, J. C. García-Quesada, I. Martin-Gullon, M. G. Montalbán, *Polymers* **2019**, *11*, 1084.
- [79] M. I. J. Ibrahim, S. M. Sapuan, E. S. Zainudin, M. Y. M. Zuhri, *Int. J. Food Prop.* **2019**, *22*, 925.
- [80] E. D. Cranston, D. G. Gray, *Biomacromolecules* **2006**, *7*, 2522.
- [81] Nanocrystalline Cellulose, Its Preparation and Uses of Such Nanocrystalline Cellulose Patent. *US 2017/0306056 A1*; *EP 3204428*; *CA 2963698*, <https://data.epo.org/gpi/EP3204428B1>, **2017**.
- [82] J. S. Alves, K. C. Dos Reis, E. G. T. Menezes, F. V. Pereira, J. Pereira, *Carbohydr. Polym.* **2015**, *115*, 215.
- [83] International Standardization Organization, ISO 527-1:2019, Plastics – Determination of Tensile Properties – Part 1: General Principles, (2019). <https://www.iso.org/standard/75824.html> (accessed: April 2021).